

EVALUATION OF PIER-SCOUR PREDICTIONS FOR WIDE PIERS USING FIELD DATA

Nordila Ahmad¹, Bruce W. Melville², Thamer Mohammad³, Zuliziana Suif¹

¹Faculty of Engineering, National Defence University, Malaysia; ²Faculty of Engineering, The University of Auckland, Auckland; ³College of Engineering, University of Baghdad, Iraq

*Corresponding Author, Received: 14 May 2017, Revised: 29 Nov. 2017, Accepted: 28 Dec. 2017

ABSTRACT: Many research have been carried out and formulas derived to estimate wide pier scour equation. However, many of these formulas were derived using data from laboratory and very limited equation that had been developed were tested using data from field. The purpose of this paper is to evaluate the laboratory wide pier scour equation that proposed from the previous findings with field data set. Large number of field data from the literature were extracted and it consist both clear-water and live-bed scour. A technique for evaluating the quality of the data was created and tested to the data set. Three pier-scour equations of wide pier from the literature also used to analyze the performance of each equation. Comparisons of computed and measured scour depths show that the formula from the previous publication demonstrated the smallest discrepancy ratio and Root Mean Square Error value when compared with the large number of laboratory and data from field.

Keywords: Local scour, Field data, Wide piers, Scour equation

1. INTRODUCTION

Scour is the lowering of the riverbed level due to erosion of water where this phenomenon is tend to expose the bridge foundations. The extent of this reduction below an assumed natural level is termed the *depth of scour* or *scour depth*. The basic mechanism that causes local scour around piers is the downflow at the upstream side of the pier and the vortex formation at the bed. The flow moves more slowly as it move toward to the pier, coming to a rest at the pier face. The approach flow velocity is diminished to zero at the side of the upstream pier and this result in a pressure increase around the pier face. The associated pressures are extreme near the surface, where the rate of decrease in velocity is greatest, and becomes lower the closer the flow is to the river bed [17]. As the velocity decreases the closer the flow is to the river bed, the pressure on the pier face also reduce accordingly, creating a downward pressure gradient. Next, the pressure gradient forces the flow down the pier face, and it is look like a vertical jet. The downflow process gives an effect on the river bed and produce a scour hole around the base of pier. The downflow impinging on the streambed is the major scouring agent [17], [15], [11]. Fig. 1 shows the scour pattern and flow around circular pier.

Actually, the flow field surrounding a pier structure is quite complicated and complex, even for structures with simple pier such as piers with a circular shape. One of the main characteristics of the local flow field is the development of secondary

flows called vortices. Many researchers [12], [13], [7] have proposed that these vortices are the most significant mechanisms of local scour.

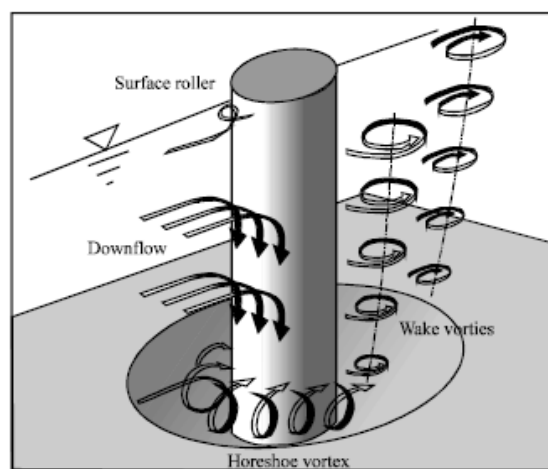


Fig. 1 The scour pattern and flow around circular bridge pier

2. PARAMETERS AFFECTING LOCAL SCOUR AROUND BRIDGE PIERS

In order to measure the relationship between the local scour depth around bridge pier and its dependent parameters, a comprehensive discussion of the mechanics of local scour around bridge piers was presented. [6] noted the relationship between the local scour depth at a bridge pier and its dependent parameters, which can be stated as:

$$d_s = f[\text{Flood flow}(\rho, \nu, U, g, y), \text{Bed sediment}(d_{50}, \sigma_g, \rho_s, U_c), \text{Bridge geometry}(Al, Sh, b), \text{Time}(t)] \quad (1)$$

where ν and ρ = kinematic viscosity and fluid density, respectively; U = mean approach flow velocity; g = acceleration of gravity; y = flow depth; σ_g and d_{50} = geometric standard deviation of the sediment particle size distribution and median size, respectively; ρ_s = sediment density; b = pier width; U_c = critical mean approach flow velocity for entrainment of bed sediment; Al and Sh = parameters describing the alignment of the pier and shape (including floating debris), respectively; t = time; and f denotes "a function of".

By assuming a constant relative density of sediment, for example by neglecting ρ , and ρ_s , and ν , Eq. (2) can be written as:

$$\frac{d_s}{b} = f\left(\frac{U}{U_c}, \frac{y}{b}, \frac{b}{d_{50}}, \sigma_g, Sh, Al, \frac{Ut}{b}, \frac{Ub}{\nu}\right) \quad (2)$$

The first three parameters on the right-hand side of Eq. (2) are flow-related and represent, respectively, the phase of sediment transport on the approach flow bed (flow intensity), the depth of flow relative to the size of the foundation (flow shallowness), and the foundation size relative to the sediment median size (sediment coarseness). The last two terms is a time scale for the development of scour (Ut/b) and the effect of viscosity (Ub/ν) based on the size of the foundation.

The rationale of choosing that dimensionless parameters in this study is, all of those parameters were used in pier analyses.

3. PREVIOUS FORMULAS FOR WIDE PIER LOCAL SCOUR

In terms of wide and long skewed piers, many empirical local scour prediction formulas overestimate depths of scour around wide structures compared to the depths of water where they are built. The equations were developed using laboratory data from experiments of steady flow. Due to the complexity of the sediment transport and flow associated with processes of local scour, there are a large of dimensionless class required to fully characterise the scour. Most of these class, such as the ratio of water depth to structure diameter (y/b), can be kept constant between the model from laboratory and the prototype structure. Nevertheless, as there is a lower limit on the sediment particle size before cohesive forces become crucial, those class involving sediment size cannot be kept constant between the prototype and model [1]. If the sediment-to-structure-length scales are not correctly calculated for in the predictive formulas, problems

will occur when the formulas are used in conditions which differ from the laboratory situations on which they are built. The problems will be related to the model not being able to maintain the proper scale between model and prototype sediment as the size of the prototype structure increases [1]. This condition always occurs in huge gravity structures such as in the case of large coastal and inland bridge piers.

The problem in wide pier is usually considered to be a concern when the relative depth, y/b , is too small to allow the vortices to fully develop. Earlier investigations of the dependence of depth of scour (y/b) were executed with very shallow water depths and small piles [7]. [5] established an upper threshold at $y/b = 3$ beyond which the depth of scour is relatively independent of the relative depth. However, [1] conducted experiments with large piers which indicate that the threshold should be closer to 2, although data below these thresholds are included in a number of empirical formulas that overestimated prototype scour depths. There are various researchers who have attempted to deal with this problem.

HEC-18 [3] is the standard used by many highway agencies for evaluating scour at bridges. It was determined from a plot of laboratory data for circular piers. In the latest edition of HEC-18 [9], the HEC-18 pier scour formula (based on the CSU formula) is recommended for both clear-water and live-bed pier scour. The formula forecast maximum pier scour depths. The new formula of HEC-18 [9] is shown in Eq. (3).

$$\frac{d_s}{b} = 2K_1 K_2 K_3 \left(\frac{y}{b}\right)^{0.35} Fr^{0.43}$$

where

- d_s = scour depth (m)
- y = flow depth directly upstream of the pier, (m)
- K_1 = correction factor for pier nose shape
- K_2 = correction factor for angle of attack of flow
- K_3 = correction factor for bed condition
- b = pier width (m)
- Fr = Froude Number directly upstream of the pier, $U/(gy)^{1/2}$, where, U =mean velocity of flow directly upstream of the pier, (m/s)

Jones and Sheppard equations [1] include the b/d_{50} ratio and thus should be directly applicable to large structures (wide piers). They concluded that the pier width affects the equilibrium scour depth in two methods. First, the ratio of pier size to flow depth (y/b) is vital and can best be represented by a function of hyperbolic tangent, which creates the depth of scour primarily a function of the pier size for relatively slender piers, but a function of the flow

depth for relatively wide piers. Second, the ratio of pier size to sediment (b/d_{50}) can give an even greater impact on the scour prediction. Moreover, they have demonstrated that the maximum relative clear-water scour happen when the ratio of b/d_{50} is about 46, and that scour tends to reduce on both sides of this value for constant values of U/U_c and y/b (Fig 2). The equation produced by Jones and Sheppard is shown in Eq. (4).

$$\frac{d_s}{b} = c_1 \left[\frac{5}{2} \left(\frac{U}{U_c} \right) - 1 \right]$$

where

$$c_1 = \frac{2}{3}k \quad \text{and}$$

$$k = \frac{\tanh \left[2.18 \left(\frac{y}{b} \right)^{0.66} \right]}{\left[-0.279 + 0.049 e^{\left(\log_{10} \left(\frac{b}{d_{50}} \right) \right)} + \frac{0.78}{\log_{10} \left(\frac{b}{d_{50}} \right)} \right]}$$

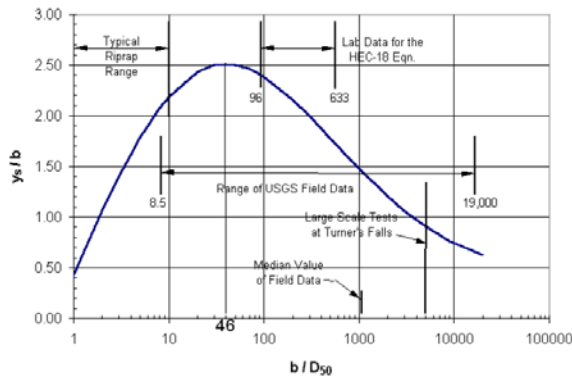


Fig. 2 Dependence of normalised depth of scour on b/d_{50} for a circular pier. The graph shown $U/U_c=1$ and $y/b>2$

Based on a recent publication, [10] have made an improvement in developing the best-performing equations. The recommended equilibrium local scour equation resulting from their study is a combination of equations developed by [2] and [4], and is referred to as the Sheppard/Melville or S/M equation. [10] concluded that the predictive methods have improved in accuracy over the years, with those developed in recent years demonstrating the best performance. The Sheppard/Melville (S/M) method was found to be the most accurate of those tested and is recommended for use in design. The S/M equation is shown in Equation 2.27.

$$\frac{d_s}{b^*} = 2.5 f_1 f_2 f_3 \quad \text{for } 0.4 < U/U_c < 1 \quad (5)$$

where

$$f_1 = \tanh \left(\frac{y}{b^*} \right)^{0.4},$$

$$f_2 = \left\{ 1 - 1.2 \left[\ln \left(\frac{U}{U_c} \right) \right]^2 \right\}, \text{ and}$$

$$f_3 = \frac{\left(\frac{b^*}{d_{50}} \right)}{\left[0.4 \left(\frac{b^*}{d_{50}} \right)^{1.2} + 10.6 \left(\frac{b^*}{d_{50}} \right)^{-0.13} \right]}$$

where

$$b^* = b_p \phi$$

b^* = effective pier width;

b_p = projected pier width;

ϕ = 1.0 for a circular pier;

and

$$\phi = 0.86 + 0.97 \left[\theta - \frac{\pi}{4} \right]^4$$

for a skewed pier

4. EVALUATION OF LABORATORY-DERIVED CURVE ON FIELD DATA

[16] present the relationship between equilibrium local scour depth (d_s/b) and sediment coarseness for large ranges of b/d_{50} . Analysis of least-squares regression using a fitting criterion of mean square error was used to all data in their study plus with laboratory data in the literature, and found the optimum coefficients which reduced the mean square error between the experimental and predicted values. The best fit correlation between b/d_{50} and d_s/b is presented by this laboratory-derived curve in Eq. (6) and the graph can be shown in Fig. 3.

$$\frac{d_s}{b} = 3.4 - \frac{30}{\left(\frac{b}{d_{50}} \right)} \exp \left[0.088 \left(\ln \left(\frac{b}{d_{50}} \right) \right)^2 \right] \quad (6)$$

In this study, the field measurements of [14] were used to test the applicability of Eq. (6) to field data. The measurements consist of both clear-water and live-bed data sets. Before the comparison was made, the field data were filtered from 493 to 45 data sets. This is because when the full data set is used, there is no relationship obtained between d_s/b and b/d_{50} . Therefore, several steps had been taken in

choosing the field data. First, only a single pier type was selected. Second, data that $b/d_{50} > 50$ were chosen [8].

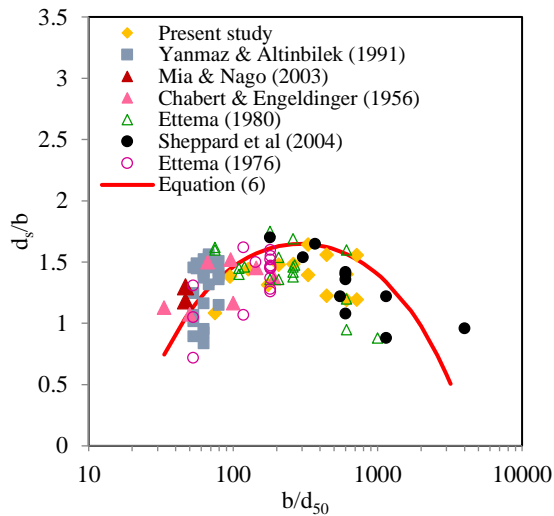


Fig. 3 Plot of d_s/b versus b/d_{50} from laboratory data [16]

Thirdly, the data points that have $d_{50} < 0.1$ mm were eliminated in order to consider the cohesive effects from that sediment. Fourth, data that affected from debris accumulation around the bridge pier were also eliminated due to there being no definite relationship between the scour depth and debris accumulation. Fifth, if the scour depth was measured at the upstream and downstream of the bridge pier, only the maximum value of scour depth was preferred. Finally, if the scour depth was measured around the same bridge pier, only the maximum scour depth was chosen. This gives 15 data sets from clear-water scour conditions and 30 data sets from live-bed conditions. All of the filtered data are graphically shown in Fig. 4 along with the best fit curve from Fig. 3.

According to Fig. 4, most of the clear-water field data indicate reasonable agreement with the laboratory-derived curve when it is considered as an upper envelope curve. For those clear-water scour data sets below the curve, it may be that pier scour depth could not attain the equilibrium stage during the time in which the data were measured because of the short duration of the flood relative to the equilibrium time. Regardless, it can be considered that uncertainty occurs during measurement of scour and it is never known whether the bed has attained an equilibrium stage during scour data measurements. Similar

Although the recorded scour depth can represent equilibrium scour conditions for live-bed scour, it is possible that the recorded scour depth was less than the equilibrium value because of the dynamic flow and sediment transport aspects around a bridge site like the transition of dunes through the scour hole.

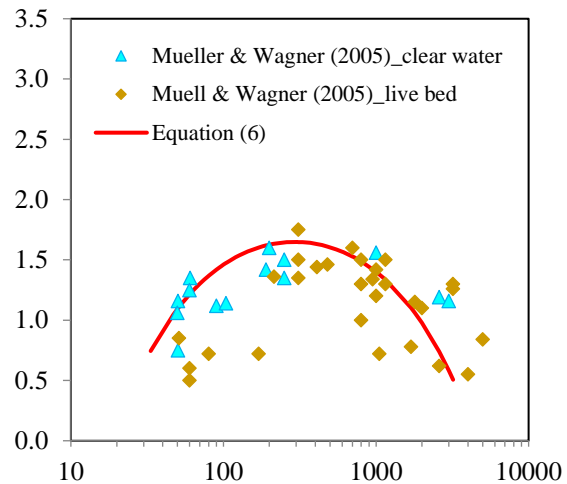


Fig. 4 Plot of d_s/b versus b/d_{50} for selected field data. (Source of data: [14])

discrepancies can occur for scour data in live-bed conditions, but this may be for other reasons.

However, the combination of the laboratory-derived curve with the field data which have been filtered as demonstrated in Fig. 4 gives evidence that the normalized scour depth appears to be significantly reduced for the large values of b/d_{50} that are frequently found in the field. It was found that Eq. (6) can fit both data sets for live-bed and clear-water conditions. For extra safety, the value acquired from Eq. (6) can be added with 25% in order to consider the value of the maximum scour depth for the all data sets used.

5. ASSESSMENT OF EXISTING EQUATIONS FOR ESTIMATING MAXIMUM LOCAL SCOUR DEPTH AROUND WIDE PIERS

In this part, in order to validate the predicted maximum scour depth at wide piers using formulas suggested by [1], HEC-18 [9], and [10], the field data sets were used. Statistical evaluation was done to determine the performance of each predictive formula. The root mean square error (RMSE), the standard deviation of the discrepancy ratio (σ_r) and the discrepancy ratio (r) were analysed. The equation for the statistical analysis are shown below:

$$RMSE = \sqrt{\frac{\sum_{i=1}^N (d_s/b_{predicted,i} - d_s/b_{measured,i})^2}{N-1}}$$

(7)

$$r = \frac{(d_s/b)_{predicted}}{(d_s/b)_{measured}} \quad (8)$$

$$\sigma_r = \sqrt{\frac{1}{N-1} \sum_{i=1}^N (r_i - \bar{r})^2} \quad (9)$$

Where \bar{r} is the mean of the discrepancy ratio. A value of unity for \bar{r} depicts best agreement between the measured values and dimensionless scour depths of the predicted. σ_r represents the assessment of the scatter in the predictions relative to the average value.

The statistical analysis using the predicted and field data sets is also shown in Table 1. It was found that all the tested equations over-predict the d_s/b values for field conditions. As stated previously, the probable reasons for this are that the field data contain non-equilibrium field scour conditions and discrete measurements rather than data based on measurements that were made continuously with time in the field. The lack of agreement with the field data sets can be attributed to the difficulty in measuring field data using flood-chasing or discrete measurement in time without being able to take into account the unsteady development of the scour hole itself. Therefore, it is likely that the proposed equation will produce the smallest RMSE value and discrepancy ratio when compared with the large number of field and laboratory data. The scattergrams or visual comparison is another way that can be used to assess the predictive formulas using the measured and predicted scour depths around wide piers. Fig. 5 show the dimensionless scour depth for field data sets. The plot demonstrate how many the predicted values of normalised scour depth deviate from the perfect agreement line. From the observation, the results acquired from using Eq. (6) are found to be in agreement with the results acquired from applying the selected formulas during data sets from field are used.

Table 1. Data of the root mean square error, RMSE and discrepancy ratio, r , for each predictive formula

	Field data		
	r		
	\bar{r}^3	σ_r^2	RMSE ¹
Jones and Sheppard (2000)	2.75	3.43	1.21
HEC-18 (2012)	6.26	7.95	4.22
Sheppard et al. (2014)	2.68	3.43	0.99
Present study	2.54	3.01	0.80

RMSE¹ = root mean square error, σ_r^2 = standard deviation of discrepancy ratio, \bar{r}^3 = average discrepancy ratio,

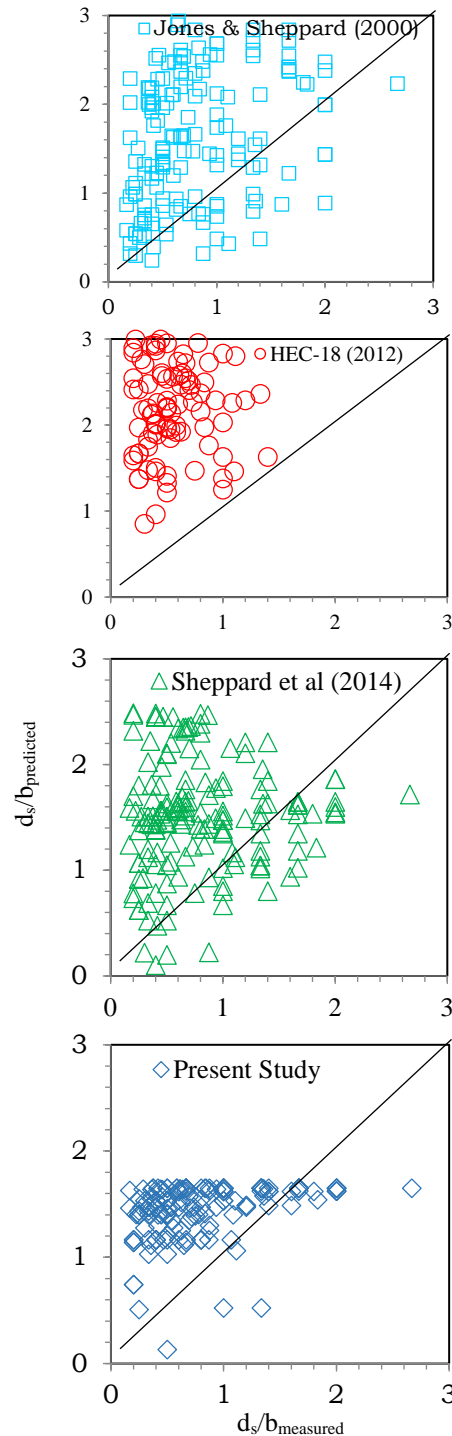


Fig. 5. Comparison of the measured and predicted normalized scour depths in the field [14] with selected existing scour depth predictive equations

6. CONCLUSION

In order to show the effectiveness of the proposed equation from the previous findings [16] for predicting maximum scour depth around wide piers, several scour prediction equations were evaluated with field data. It was found that equations from [1], [9] and [10] mostly over-predict scour depth, as

shown by the statistical analysis with the discrepancy ratio, r , and RMSE in Table 1. This evaluation was also supported by scattergrams, shown in Fig. 5. Equation (6) shows the lowest RMSE and discrepancy ratio, r , and thus can be reliably used to estimate depth of scour at the prototype scale. As a factor of safety, the value acquired from Eq. (6) can be added with 25% in order to consider the value of the maximum scour depth for the all data sets used.

For the present, it needs to be emphasized that the applicability of Eq. (6) is limited to values of b/d_{50} from 50 – 4200, to skewed piers with angle of attack, $\alpha < 45^\circ$, to graded sediments with σ_g less than 7 and to piers in shallow flows.

7. ACKNOWLEDGEMENTS

The financial support from the Short Term Grant given by National Defence University, Malaysia (Grant No. J0033-UPNM/2015/GPJP/2/TK/03) for this project is acknowledged. The experiments were conducted in the Hydraulic Laboratory in the National Hydraulic Research Institute of Malaysia (NAHRIM).

8. REFERENCES

- [1] Jones, J. Sheppard, D. 2000, Scour at wide bridge pier. *Building Partnerships*, pp. 1–10.
- [2] Melville, B. W. (1997). "Pier and abutment scour: Integrated approach." *Journal of Hydraulic Engineering-ASCE*, 123(2), 125–136.
- [3] Richardson, E. V., and Davis, S. R. (2001). "Evaluating scour at bridges." Fourth Edition. Hydraulic Engineering Circular No. 18 (HEC-18), Federal Highway Administration, Washington, D.C.
- [4] Sheppard, D.M., Miller, W., 2006. Live-bed local pier scour experiments. *Journal of Hydraulic Engineering*, ASCE, 132(7), 635–642
- [5] Melville, B. W., and Sutherland, A. J. (1988). "Design method for local scour at bridge piers." *Journal of Hydraulic Engineering-ASCE*, 114(10), 1210–1226.
- [6] Melville, B.W., Coleman, S.E., 2000. *Bridge Scour*. Water Resources Publications, LLC, Colorado, U.S.A., 550 p.
- [7] Ettema, R., 1980. Scour around bridge piers. Report No. 216, University of Auckland, Auckland, New Zealand.
- [8] Sheppard, D. M. (2004). "Overlooked local sediment scour mechanism." *Transportation Research Record: Journal of the Transportation Research Board*, 1890, 107–111.
- [9] Arneson, L. A., Zevenbergen, L. W., Lagasse, P. F., and Clopper, P. E. (2012). Evaluating scour at bridges, 4th Ed. Hydraulic Engineering Circular No. 18 (HEC-18), Federal Highway Administration, Washington, DC
- [10] Sheppard, D. M, Huseyin, D. Melville. B. W. (2014). Evaluation of Existing Equations for Local Scour at Bridge Piers. *Journal of Hydraulic Engineering-ASCE*, 140(1), 14–23
- [11] Ibrahimy M. I. and S. M. A. Motakabber. Bridge Scour Monitoring by Coupling Factor Between Reader and Tag Antennas of RIFD System. *International Journal of GEOMATE*, 8(2), 1328-1332
- [12] Shen, H. W., Schneider, V. R., and Karaki, S. (1966). Mechanics of local scour, U.S. Dept. of Commerce, National Bureau of Standards, Institute for Applied Technology, Fort Collins, CO.
- [13] Melville, B. W. (1975) "Local Scour at Bridge Sites." Rep. No.117, School of Engineering, The Univ. of Auckland, New Zealand.
- [14] Mueller, D. S., and Wagner, C. R. (2005). "Field observations and evaluations of streambed scour at bridges." Office of Engineering Research and Development, Federal Highway Administration, McLean, Virginia.
- [15] Dey, S. (1996). "Sediment pick-up for evolving scour near circular cylinders." *Applied Mathematical Modelling*, 20(7), 534-539.
- [16] Nordila A., Thamer A. M. and Zuliziana S. (2016). "Prediction of Local Scour around Wide Bridge Piers under Clear-water Conditions". *International Journal of GEOMATE*, June, 2017, Vol 12 Issue 34, pp. 135-139
- [17] B.W. Melville, A.J. Raudkivi (1977). "Flow characteristics in local scour at bridge piers". *Journal of Hydraulic Research*, 15 (4) (1977), pp. 373-380

Copyright © Int. J. of GEOMATE. All rights reserved, including the making of copies unless permission is obtained from the copyright proprietors.
